Dynamics of Translesion DNA Synthesis Catalyzed by the Bacteriophage T4 Exonuclease-Deficient DNA Polymerase†

Anthony J. Berdis*

Department of Pharmacology, School of Medicine, Case Western Reserve University, 10900 Euclid Avenue, Cleveland, Ohio 44106

Received January 24, 2001; Revised Manuscript Received April 12, 2001

ABSTRACT: The mechanism and dynamics of translesion DNA synthesis were evaluated using primer/templates containing a tetrahydrofuran moiety designed to mimic an abasic site. Steady-state kinetic analysis reveals that the T4 DNA polymerase preferentially incorporates dATP across from the abasic site with 100-fold higher efficiency than the other nucleoside triphosphates. Under steady-state conditions, the catalytic efficiency of dATP incorporation across from an abasic site is only 220-fold lower than that across from T. Surprisingly, misincorporation across from T is favored 4−6-fold versus replication across an abasic site, suggesting that the dynamics of the polymerization cycle are differentially affected by formation of aberrant base pairs as opposed to the lack of base-pairing capabilities afforded by the abasic site. Linear pre-steady-state time courses were obtained for the incorporation of any dNTP across from an abasic site, indicating that chemistry or a step prior to chemistry is rate-limiting for the polymerization cycle. Low elemental effects (<3) measured by substituting the α-thiotriphosphate analogues for dATP, dCTP, and dGTP indicate that chemistry is not solely rate-limiting. Single-turnover experiments yield k_{pol}/K_d values that are essentially identical to k_{cat}/K_m values and provide further evidence that the conformational change preceding chemistry is rate-limiting. Extension beyond an A:abasic mispair is approximately 20-fold and 100-fold faster than extension beyond a G:abasic mispair or C:abasic mispair, respectively. Extension from the G:abasic or A:abasic site mispair generates significant elemental effects (between 5 and 20) and suggests that chemistry is at least partially rate-limiting for extension beyond either mispair.

The proper action of DNA replication as well as its coordination with other biological processes is thus essential to maintain the integrity of an organism's genomic material in order for it to survive and propagate. It is well established that the functional groups of nucleobases are required for proper hydrogen-bonding interactions that dictate their base-pairing capabilities. Unfortunately, these functional groups are also very reactive and can be modified by a variety of electrophilic and nucleophilic compounds (reviewed in *1*). These modifications can alter the hydrogen-bonding capabilities and can lead to the introduction of genomic mutations caused by proper base-pairing during DNA replication. To fully define the underlying mechanism of mutagenesis and disease development, it is necessary to understand the *mechanism* of nucleotide discrimination when damaged templates are encountered by the DNA replication apparatus. By contrasting the mechanism of precise versus mutagenic DNA replication, the physiological *consequences* of altered DNA replication can then be fully understood.

A wide variety of DNA lesions known to induce errors in DNA replication have been identified both in vitro and in vivo (reviewed in *2*). Perhaps the most prevalent and damaging of these DNA lesions is an apurinic/apyrimidinic (abasic)[1] site. Although abasic sites arise spontaneously under normal physiological conditions (*3*), their formation is enhanced by exposure to ionizing radiation and certain chemicals (*4*) as well as through the action of DNA glycosylases which act to excise damaged nucleobases (*5*). While most abasic DNA lesions are removed by a base excision repair pathway (*5*), a small fraction of lesions persist and are replicated to yield a high probability of mutagenesis (*6*). Since no coding information is present at an abasic site, there exists a 75% chance of incorporating the wrong nucleotide to yield a genetic mutation. However, it has been demonstrated in a variety of DNA replication systems (*7*−*9*) that dAMP is preferentially incorporated across from an abasic site, and this phenomenon has been coined the "A-rule" (*7*−*9*).

In this report, the mechanism and dynamics of translesion DNA synthesis were evaluated using the bacteriophage T4 DNA polymerase as a model system as this enzyme is one of the least error-prone polymerases, exhibiting an in vivo frequency of misincorporation of 1 in 10^8 turnovers (*10*). The extraordinary degree of fidelity arises from a multiplicative process in which the polymerase has at least four

† This research was supported through funding from the American Cancer Society (IRG-91-022-06-IRG) to the Cancer Center at Case Western Reserve University and University Hospitals.

* Corresponding author. Telephone: (216)-368-6255, Fax: (216)-368-6255, e-mail: ajb15@po.cwru.edu.

[1] Abbreviations: abasic, apurinic/apyrimidinic; TBE, Tris-HCl/borate/EDTA; EDTA, ethylenediaminetetraacetate, sodium salt; dNTP, deoxynucleoside triphosphate; α-S-dNTP, deoxynucleoside 5′-O-(3-α-thiotriphosphate).

10.1021/bi0101594 CCC: $20.00
Published on Web 05/23/2001

Scheme 1: Different Kinetic Steps Associated with the Maintenance of Fidelity[a]

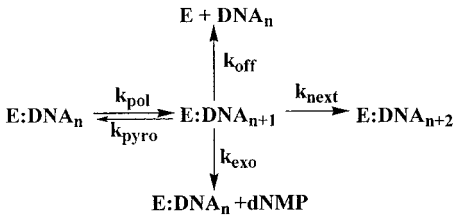

[a] k_{pol} refers to the rate of DNA polymerization in extending DNA$_n$ to DNA$_{n+1}$, k_{pyro} refers to the rate of pyrophosphorolysis (reversal of DNA polymerization), k_{next} refers to the rate of DNA polymerization in extending DNA$_{n+1}$ to DNA$_{n+2}$, k_{off} refers to the rate of enzyme dissociation from the DNA substrate, and k_{exo} refers to the rate of exonucleolytic degradation of DNA$_{n+1}$ to yield DNA$_n$.

opportunities to discriminate against errors during synthesis (Scheme 1).

The first control point for accuracy is the binding of correct dNTP to the DNA-bound polymerase (*11*). A subsequent conformational change in the enzyme is proposed to align the incoming dNTP into a precise geometrical configuration for phosphoryl transfer and constitutes an additional kinetic point for error discrimination (*11*). This induced-fit mechanism imposes discrimination against misincorporation as premutational intermediates disrupt or alter the geometry of the polymerase's active site to prevent extension of the primer. In the case of the T4 DNA polymerase, these two steps provide an error frequency of 1 misincorporation per 10^5-10^6 turnovers (*11*). A third level of error discrimination arises from proofreading by the enzyme's 3′→5′ exonuclease activity which removes misincorporated nucleotides to regenerate a correctly base-paired primer/template to reduce the error frequency a further 10^2-10^3-fold (*11*). A fourth level of discrimination arises from the ability of the polymerase to dissociate from a primer/template containing a 3′-terminal mispair and preferentially continue DNA synthesis on a correct primer/template.

The dynamics of these processes toward maintaining fidelity have been extensively studied on a variety of DNA polymerases focusing on the importance of hydrogen-bonding capabilities of potential base pairs to explain alterations in kinetic steps along the reaction pathway (*12*−*16*). However, the nature of the abasic DNA lesion is significantly different from other DNA lesions that possess hydrogen-bonding capabilities. Indeed, the results presented here from steady-state, pre-steady-state, and single-turnover kinetic analyses demonstrate that the dynamics by which the DNA polymerase discriminates against dNTP incorporation are different upon encountering this unique DNA lesion. The importance of several enzyme-mediated steps in hindering incorporation across from and beyond an abasic site is discussed within the context of the solution structures of DNA containing the four nucleosides across from an abasic site (*17*, *18*).

MATERIALS AND METHODS

Materials

[γ-^{32}P]ATP and [α-^{32}P]dATP were purchased from New England Nuclear. Unlabeled dNTPs (ultrapure) and unlabeled ddGTP and ddATP (ultrapure) were obtained from Pharmacia. $MgCl_2$, $Mg(OAc)_2$, and all buffers were from Sigma. All other materials were obtained from commercial sources and were of the highest available quality. Oligonucleotides, including those containing a tetrahydrofuran moiety mimicking an abasic site, were synthesized by Operon Technologies (Alameda, CA). Single-stranded and duplex DNAs were purified and quantified as described (*12*). T4 exonuclease-deficient polymerase D129A (Asp-219 to Ala mutation) was purified and quantified as previously described (*19*).

Methods

The assay buffer used in all kinetic studies consisted of 25 mM Tris−OAc (pH 7.5), 150 mM KOAc, and 10 mM 2-mercaptoethanol. All assays, including rapid quench experiments using the instrument described by Johnson (*20*), were performed at 25 °C. Polymerization reactions were monitored by analysis of the products on 20% sequencing gels as described by Mizrahi et al. (*21*). Gel images were obtained with a Molecular Dynamics PhosphorImager. Product formation was quantified by measuring the ratio of ^{32}P-labeled extended and nonextended primer. The ratios of product formation are corrected for substrate in the absence of polymerase (zero point). Corrected ratios are then multiplied by the concentration of primer/template used in each assay to yield total product. All concentrations are listed as final solution concentrations.

Steady-State Incorporation Assays. The kinetic parameters, k_{cat}, K_m, and k_{cat}/K_m, for each dNTP during translesion DNA synthesis were obtained by monitoring the rate of product formation using a fixed amount of T4 exo$^-$ polymerase (10 nM) and DNA substrate (1000 nM) at varying concentrations of dNTP (0.01−5 mM). Aliquots of the reaction were quenched into EDTA (0.5 M, pH 7.4) at variable times (5−600 s). Samples were diluted 1:1 with sequencing gel load buffer, and products were analyzed for product formation by denaturing gel electrophoresis. In all cases, steady-state rates were obtained from the linear portion of the time course. Data obtained for steady-state rates in DNA polymerization measured under pseudo-first-order reaction conditions were fit to eq 1:

$$y = mt + b \quad (1)$$

where m is the slope of the line, b is the y-intercept, and t is time. Data for the dependency of k_{obs} as a function of dNTP concentration were fit to the Michaelis−Menten equation:

$$k_{obs} = k_{pol}[\text{dNTP}]/K_m + [\text{dNTP}] \quad (2)$$

where k_{obs} is the observed first-order rate constant, k_{pol} is the rate of DNA polymerization, K_m is the Michaelis constant for dNTP, and [dNTP] is the concentration of nucleotide substrate.

Pre-Steady-State Nucleotide Incorporation Assays. The kinetics of dNTP incorporation were examined using either 13/20$_T$-mer or 13/20SP$_T$-mer. A preincubated solution of 200 nM T4 exo$^-$ polymerase and 1000 nM 5′-labeled DNA was mixed with an equal volume of a solution containing 10 mM magnesium acetate and 200 μM dATP in the same reaction buffer. The reaction was then terminated at various times by the addition of 500 mM EDTA. Polymerization products were analyzed as described above. The measured rates for

Scheme 2: Simplified Reaction Mechanism Representing the Sequential Conversion of Potential Substrates into Products during Replication beyond a dNMP:Abasic Site Mispair[a]

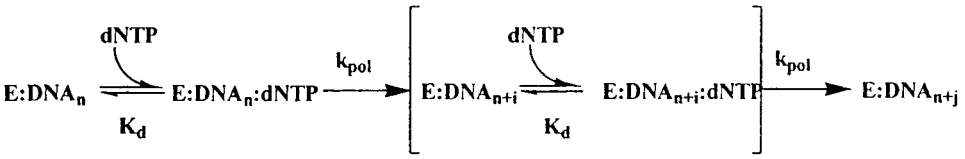

[a]In this mechanism, the rate and amount of product formation are dependent upon the equilibrium dissociation constant (K_d) for dNTP and k_{pol}, the rate of DNA extension. k_{pol} combines the kinetic steps encompassing the conformational change prior to phosphoryl transfer, phosphoryl transfer, the conformational change after phosphoryl transfer, and pyrophosphate release. Kinetic steps reflecting enzyme dissociation and rebinding to product DNA are assumed to be negligible since the reactions were performed using enzyme in a 4-fold excess versus DNA substrate.

incorporation across from the abasic site were fit to eq 1. Data were also fit to eq 3 which defines a burst in product formation followed by a steady-state rate:

$$y = Ae^{-kt} + Bt + C \quad (3)$$

where A is the burst amplitude, k is the first-order rate constant, B is the steady-state rate, t is time, and C is a defined constant.

Determination of the Equilibrium Dissociation Constant, K_d, for the 13/20SP-mer. T4 exo$^-$ polymerase (100 nM) was incubated with 13/20SP-mer (12.5−200 nM) in assay buffer containing EDTA (100 μM) and mixed with dATP (100 μM) containing magnesium acetate (10 mM) in assay buffer. The reactions were quenched with EDTA (500 mM) at variable times (5−300 s) and were analyzed as described above. The K_d for DNA substrate was obtained using the quadratic equation:

$$\text{E:DNA} = 0.5(K_d + [\text{E}] + [\text{DNA}]) - [0.25(K_d + [\text{E}] + [\text{DNA}])^2 - \text{E:DNA}]^{1/2} \quad (4)$$

where [E] is the concentration of T4 DNA polymerase, [DNA] is the concentration of 13/20SP-mer, E:DNA is the burst amplitude, and K_d is the equilibrium binding constant for DNA.

Single-Turnover Nucleotide Incorporation Assays. T4 exo$^-$ polymerase (1 μM) was incubated with 250 nM DNA (13/20SP-mer or 13/20-mer) in assay buffer containing EDTA (100 μM) and mixed with variable concentrations of dNTP (0.01−5 mM) and 10 mM $Mg(OAc)_2$. The reactions were quenched with 500 mM EDTA at variable times (5−900 s) and analyzed as described above. Data obtained for single-turnover DNA polymerization assays were fit to eq 5:

$$y = Ae^{-kt} + C \quad (5)$$

where A is the burst amplitude, k is the first-order rate constant, t is time, and C is a defined constant. Data for the dependency of k_{obs} as a function of dNTP were fit to the Michaelis−Menten equation to obtain values of k_{pol} and K_d for dNTP.

Inhibition by ddNTPs. T4 exo$^-$ (1 μM) was preincubated with 250 nM 13/20SP$_T$-mer and 10 mM $Mg(OAc)_2$ followed by the addition of varying concentrations of ddATP (0−400 μM) or ddGTP (0−600 μM). After a 5 s delay, 25 μM dATP was then added to initiate DNA synthesis. The reactions were quenched with 500 mM EDTA at variable times (5−900 s) and analyzed as described above. Data were fit to the equation for a single-exponential process (eq 5). The reciprocal rate constants ($1/k_{obs}$) were plotted versus the concentration of ddNTP to yield apparent K_i values for ddATP and ddGTP. True K_i values for ddATP and ddGTP were obtained using eq 6:

$$\text{app}K_i = K_i(1 + S/K_s) \quad (6)$$

where appK_i is the apparent inhibition determined through Dixon plot analysis, K_i is the true inhibition constant, S is the concentration of dATP, and K_S is the equilibrium dissociation constant for dATP.

Extension beyond an Abasic Site. Single-turnover conditions were used to measure the rates of extension beyond an A:abasic site base pair. T4 exo$^-$ polymerase (1 μM) was incubated with 250 nM DNA (14/20SP-mer) in assay buffer containing EDTA (100 μM) and mixed with variable concentrations of dNTP (0.01−5 mM) and 10 mM $Mg(OAc)_2$. The reactions were quenched with 500 mM EDTA at variable times (5−900 s) and analyzed as described above. Data were fit to the equation for a single-exponential process (eq 5).

Simulations modeling the observed kinetic time courses for nucleotide incorporation were performed by mathematical analyses using KINSIM (*22*). For analysis of multiple dNTP incorporation obtained under single-turnover conditions, a simplified mechanism depicted in Scheme 2 was employed. Both the starting reactant concentrations and the rate constants were supplied for each step of the mechanism. In all cases, the rate constants were based either upon experimentally determined rate constants or on published literature values. The simulated curves were then compared to those experimentally derived to judge how accurately the set of rate constants simulate the experimental data. Adjustments to the rate constants are then made until the simulated time courses are nearly identical to the experimental time courses. The iterative nonlinear regression analysis program FITSIM was then used to predict how well the mechanism and the set of rate constants describe the experimental data.

RESULTS

Steady-State Kinetic Analyses. The efficiency of translesion DNA synthesis catalyzed by the bacteriophage T4 DNA polymerase was quantified by monitoring the time-dependency in the production of extended primer. Defined DNA substrates containing an abasic site in the template strand (Figure 1) were utilized to facilitate direct comparison of the mechanism controlling translesion synthesis with that of correct and incorrect DNA synthesis (*11*, *23*). Steady-state rates of nucleotide incorporation were measured using 10 nM polymerase, 500 nM 13/20SP$_T$-mer, and a fixed con-

13/20$_T$-MER

```
5′-TCGCAGCCGTCCA
3′-AGCGTCGGCAGGTTCCCAAA
```

13/20SP$_T$-MER

```
5′-TCGCAGCCGTCCA
3′-AGCGTCGGCAGGTSpCCCAAA
```

13/20SP$_C$-MER

```
5′-TCGCAGCCGTCCG
3′-AGCGTCGGCAGGCSpCCCAAA
```

12/20$_T$-MER

```
5′-TCGCAGCCGTCC
3′-AGCGTCGGCAGGTTCCCAAA
```

12/20SP$_T$-MER

```
5′-TCGCAGCCGTCC
3′-AGCGTCGGCAGGTSpCCCAAA
```

14A/20SP-MER

```
5′-TCGCAGCCGTCCAA
3′-AGCGTCGGCAGGTSpCCCAAA
```

14C/20SP-MER

```
5′-TCGCAGCCGTCCAC
3′-AGCGTCGGCAGGTSpCCCAAA
```

FIGURE 1: DNA substrates used for kinetic analysis. SP denotes the tetrahydrofuran moiety designed to mimic an abasic site.

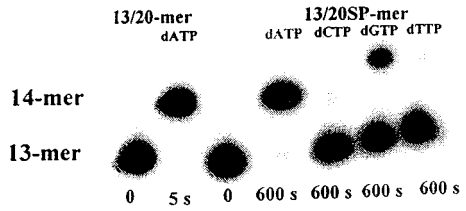

FIGURE 2: Comparison of precise versus translesion DNA synthesis catalyzed by the exonuclease-deficient bacteriophage T4 DNA polymerase. Precise DNA replication was monitored using a fixed amount of T4 exo$^-$ polymerase (50 nM), 13/20-mer DNA substrate (500 nM), and 100 μM dATP. The reaction was quenched after 5 s with 0.5 M EDTA, and products were analyzed for product formation by denaturing gel electrophoresis. Translesion DNA synthesis was monitored using a fixed amount of T4 exo$^-$ polymerase (50 nM), 13/20SP-mer DNA substrate (500 nM), and 100 μM dNTP. The reaction was quenched after 600 s with 0.5 M EDTA, and products were analyzed for product formation by denaturing gel electrophoresis.

centration of dNTP (200 μM).[2] Figure 2 reflects the preferential incorporation of dATP across from the abasic site. The rate of dATP incorporation under these conditions is approximately 30-fold higher than dGTP incorporation and 175- and 1400-fold higher than dTTP and dCTP incorporation, respectively. These data quantitatively demonstrate that T4 exo$^-$ incorporates dATP across from the abasic site with higher efficiency when compared to the incorporation of dGTP, dCTP, and dTTP and are consistent with the "A-rule" demonstrated with a variety of DNA polymerases (*7*−*9*).

[2] This level of dNTP is at least 20 times the reported K_d values during precise DNA replication (*11*, *19*) and approximately equal to the K_m value for mismatch DNA synthesis (*23*).

Table 1: Kinetic Parameters for dNTP Incorporation Across from an Abasic Site and dNTP Misincorporation Catalyzed by T4 exo$^-$ DNA Polymerase[a]

dNTP	DNA substrate	k_{cat} (s^{-1})	K_m (μM)	k_{cat}/K_m (M^{-1} s^{-1})
dATP	13/20SP$_T$-mer	0.12 ± 0.03	80 ± 10	1500
dATP	13/20$_T$-mer	3 ± 1[b,c]	10 ± 1[c]	3.3×10^5
dCTP	13/20SP$_T$-mer	0.006 ± 0.001	220 ± 25	27
dCTP	13/20$_T$-mer	0.12 ± 0.04	980 ± 50	120
dGTP	13/20SP$_T$-mer	0.025 ± 0.003	300 ± 40	83
dGTP	13/20$_T$-mer	0.032 ± 0.008	75 ± 15	430
dTTP	13/20SP$_T$-mer	0.038 ± 0.006	1200 ± 200	32
dTTP	13/20$_T$-mer	0.12 ± 0.03	650 ± 60	180

[a] Assays were performed using 10 nM T4 exo$^-$ DNA polymerase, 1000 nM DNA substrate, and variable concentrations of dNTP in the presence of 10 mM MgOAc. [b] k_{cat} was obtained from Figure 3 by dividing the steady-state rate in nucleotide incorporation by the burst amplitude which reflects functional enzyme. [c] Values reported by Frey et al. (*19*).

Steady-state assays performed using 13/20SP$_C$-mer (C replaces T at the penultimate position) also reveal a distinct preference for incorporation of dAMP versus the abasic site (data not shown). In fact, the steady-state rate of dAMP incorporation was approximately 15-fold higher than dGTP, 200-fold higher than dTTP, and 1500-fold higher than dCTP. The similarities in preferential utilization of dATP using either 13/20SP$_T$-mer or 13/20SP$_C$-mer argue against "fraying" of the primer/template as the mechanism for enhanced dATP incorporation across from the abasic site.

Steady-State Kinetic Parameters of dNTP Incorporation Across from an Abasic Site. The kinetic parameters k_{cat}, K_m, and k_{cat}/K_m for each dNTP during translesion DNA synthesis were obtained by monitoring the rate of product formation at varying concentrations of dNTP (0.01−5 mM). The rates of nucleotide incorporation were plotted as a function of dNTP concentration, and all plots displayed saturation kinetics (data not shown). Values of k_{cat}, K_m, and k_{cat}/K_m were obtained from the fit of the data to the Michaelis−Menten equation and are summarized in Table 1. For comparison, the steady-state kinetic parameters during mismatch DNA synthesis were evaluated under identical conditions and are also summarized in Table 1.

Rapid-Quench Analysis of dNTP Incorporation Across from the Abasic Site. Rapid-quench experiments were used to unambiguously detect if there is a "burst" in incorporation across from the abasic site. As a positive control, precise DNA replication monitoring the incorporation of dATP across from T revealed a biphasic time course characterized by a rapid initial burst in product followed by a second, slower phase in product formation that represents product release and subsequent turnover of remaining substrate (Figure 3A). The burst amplitude was equal to the amount of enzyme added (100 nM) and indicates that the polymerase−DNA complex is 100% catalytically competent. The rate constant of 100 ± 10 s^{-1} obtained for k_{pol} and the k_{cat} value of 2.5 ± 0.2 s^{-1} are essentially identical to previously published values (*11*, *19*).

In contrast to the biphasic time courses observed using unmodified DNA, incorporation of dATP across from the abasic site was best defined as a linear time course (Figure 3B,C). The time course for dGTP incorporation was also

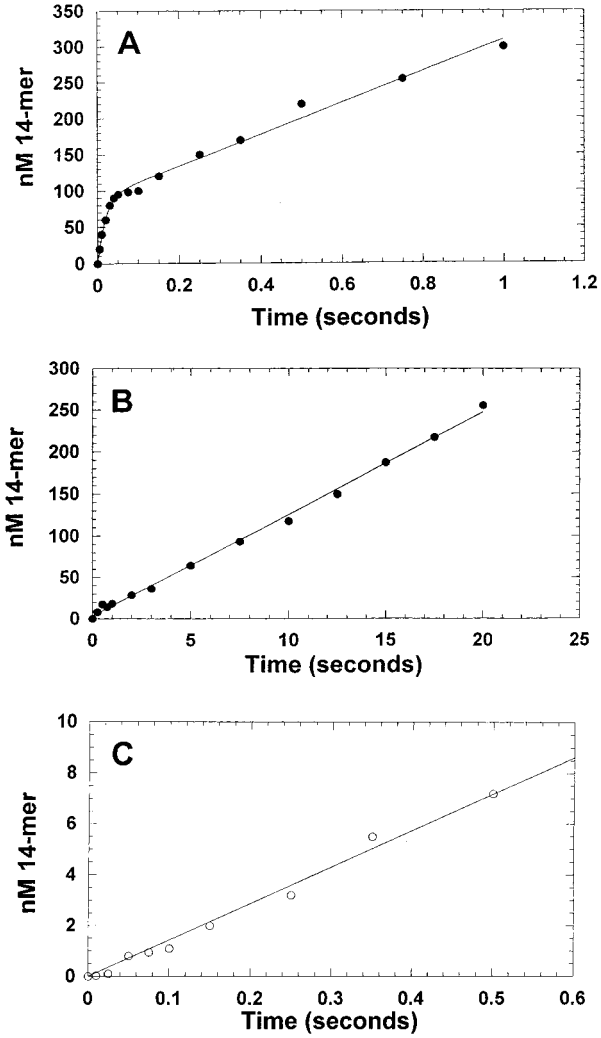

FIGURE 3: Pre-steady-state polymerization using 13/20-mer (A) or 13/20SP-mer (B and C). Assays were performed in which a preincubated solution of 200 nM T4 exo$^-$ polymerase and 1000 nM 5′-labeled DNA was mixed with an equal volume of a solution containing 20 mM MgOAc and 200 μM dATP in the same reaction buffer. The reaction was then terminated at various times by the addition of 500 mM EDTA. The solid line for the time course using 13/20-mer was obtained by fitting the data to the kinetic model described in Scheme 3. The solid line for the time course using 13/20SP-mer was likewise obtained by fitting the data to the kinetic model described in Scheme 3. However, a rate constant of 0.15 s^{-1} was used as the rate of the conformational change (Scheme 3, step 3). Panel C shows the time course of dAMP insertion with the time frame encompassing 0.01−0.5 ms. Even at short reaction times, a burst in dAMP incorporation is not detected.

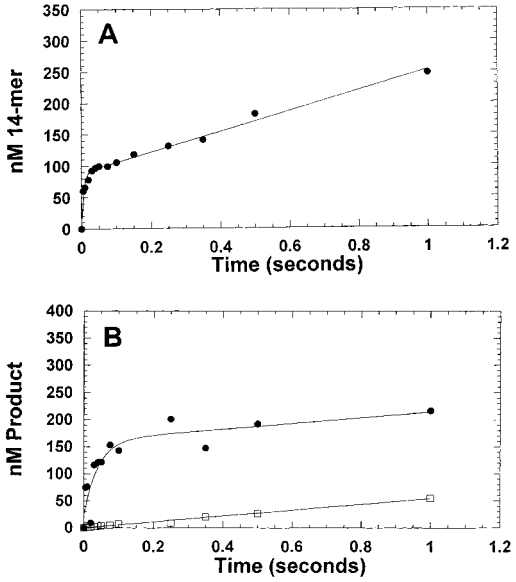

FIGURE 4: Pre-steady-state polymerization using 12/20-mer (A) or 12/20SP-mer (B). Assays were performed in which a preincubated solution of 200 nM T4 exo$^-$ polymerase and 1000 nM 5′-labeled DNA was mixed with an equal volume of a solution containing 20 mM MgOAc and 200 μM dATP in the same reaction buffer. The reaction was then terminated at various times by the addition of 500 mM EDTA. The solid line for the time course using 12/20-mer was obtained by fitting the data to the kinetic model described in Scheme 3 except that the enzyme dissociation step (step 7) was omitted and the rate of polymerization for the production of DNA_{n+1} and DNA_{n+2} was maintained at 100 s^{-1}. The solid lines for the time course using 12/20SP-mer were likewise obtained by fitting the data to the kinetic model described in Scheme 3 except that the enzyme dissociation step (step 7) was omitted. The rate constant of polymerization for the production of DNA_{n+1} (●) was maintained at 100 s^{-1} while the rate constant of polymerization for the production the DNA_{n+2} (□) was maintained at 0.2 s^{-1}.

linear (data not shown) whereas the kinetics of single nucleotide incorporation with dTTP and dCTP show slight lags (<100 ms) followed by a steady-state rate (data not shown). The lack of a defined burst using any dNTP suggests that chemistry or a step prior to chemistry is the rate-limiting step for incorporation across from an abasic site.

It has been previously reported that T4 DNA polymerase terminates DNA synthesis one nucleotide upstream from an abasic site (*24*), suggesting that the abasic site perturbs binding of enzyme to the modified DNA substrate. Similar results are reported for the pol β system in which the efficiency of incorporation across from an abasic site was higher under "running-start" conditions as opposed to "standing-start" reactions (*9*). To examine this potential mechanism, rapid-quench experiments were performed to evaluate if an abasic site affects the efficiency of incorporation at a site upstream of the DNA lesion. In these experiments, the incorporation of dATP was monitored using either the 12/20-mer or the 12/20SP-mer DNA substrate. The 12/20-mer allows the polymerase to incorporate two successive dATPs whereas the 12/20SP-mer allows the polymerase to incorporate a single dATP prior to encountering the abasic site. Using the 12/20-mer, the incorporation of dATP revealed a biphasic time course in which both dATPs were rapidly incorporated to yield DNA_{n+2} product (Figure 4A). The burst amplitude is 100 nM while k_{pol} was measured at 110 ± 12 s^{-1}. Using 12/20SP-mer, the incorporation of the first dATP was unperturbed as a burst of equal to the amount of polymerase added (100 nM) was obtained (Figure 4B). Likewise, the burst rate of 85 ± 7 s^{-1} is nearly identical to that obtained using 12/20-mer as the substrate. While the kinetics of DNA_{n+1} production were unperturbed, incorporation across from the abasic site did not reveal a burst but was instead linear as a function of time. Furthermore, the reduction in steady-state rate of 13-mer production is consistent with the enzyme binding to the newly formed 13/20SP-mer substrate but having a reduction in the rate of incorporation such that the linear time course is observed.

Single-Turnover Kinetics of Nucleotide Incorporation. Single-turnover conditions were employed to accurately measure the equilibrium dissociation constant, K_d, of the four dNTPs as well the maximal polymerization rate, k_{pol}, across

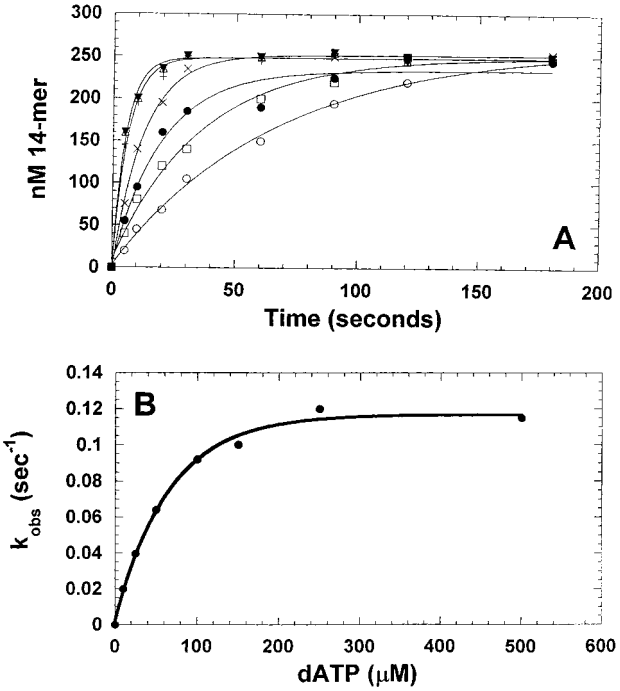

FIGURE 5: dATP concentration dependence on the apparent burst rate under single-turnover conditions. (A) T4 exo$^-$ polymerase (1 μM) and 5′-labeled 13/20SP-mer (250 nM) were preincubated, mixed with increasing concentrations of Mg^{2+}:dATP to initiate the reaction, and quenched with 500 mM EDTA at variable times (5−180 s). The incorporation of dATP was analyzed by denaturing gel electrophoresis. The dATP concentrations were 10 (○), 25 (□), 50 (●), 100 (×), 150 (+), 250 (△), and 500 μM (▼). The solid lines represent the fit of the data to a single exponential. (B) The observed rate constants for dATP incorporation (●) were plotted against dATP concentration and fit to a hyperbola to determine values corresponding to K_d and k_{pol}.

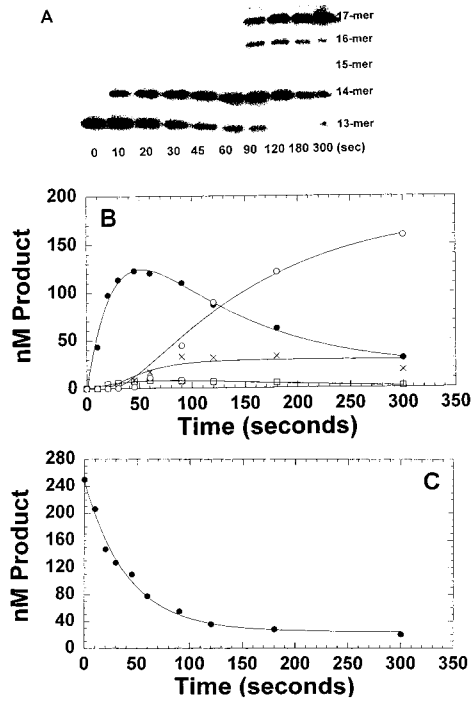

FIGURE 6: dGTP incorporation across from and beyond an abasic site. (A) T4 exo$^-$ polymerase (1 μM) and 5′-labeled 13/20SP-mer (250 nM) were preincubated, mixed with 100 μM dGTP to initiate the reaction, and quenched with 500 mM EDTA at variable times (5−180 s). The incorporation of dGTP was analyzed by denaturing gel electrophoresis. (B) Elongation of 13/20SP-mer to the 17/20SP-mer by T4 exo$^-$ polymerase showing the levels of 14- (●), 15- (□), 16- (×), and 17-mer (○). (C) The kinetics of incorporation were simplified by monitoring the depletion of 13-mer substrate as a function of time. The solid line represents the fit of the data to a single exponential.

from the abasic site. Since enzyme is in excess of DNA substrate, these experiments alleviate complications arising from any kinetic step after phosphoryl transfer and allow for the measurement of the kinetic steps reflecting initial ground-state binding of dNTP, the conformational change prior to chemistry, and/or the chemistry step itself.

Representative data displaying the concentration dependency of dATP on the rate of incorporation are presented in Figure 5. All time courses were fit to the equation for a single-exponential process to define the rate of product formation, k_{obs}. The plot of k_{obs} versus dATP concentration is hyperbolic from which values of $k_{pol} = 0.15 \pm s^{-1}$ and $K_{d\ dATP} = 35 \pm 5\ \mu$M were obtained. Similar data were obtained using dCTP or dTTP as the nucleoside triphosphate (data not shown).

Extension across from the abasic site was observed at all dGTP concentrations tested. However, under single-turnover conditions, extension beyond the abasic site was prevalent at dGTP concentrations greater than 10 μM. Because dGTP is the correct triphosphate for the next 3 incorporations, a ladder of products ranging from 14 to 17 bases was observed (Figure 6A). Despite the distribution in polymerization products, the reaction kinetics were simplified by measuring the depletion of 13-mer substrate as a function of time (Figure 6B). The plot of k_{obs} versus dGTP concentration (data not shown) yields a $k_{pol} = 0.023 \pm 0.005\ s^{-1}$ and K_d of 130 $\pm$ 20 μM. Values for k_{pol}, K_d, and k_{pol}/K_d for each dNTP are summarized in Table 2.

Table 2: Kinetic Rate and Equilibrium Constants for dNTP Incorporation Catalyzed by T4 exo$^-$ DNA Polymerase under Single-Turnover Conditions[a]

dNTP	DNA substrate	k_{pol} (s^{-1})	K_d (μM)	k_{pol}/K_d (M^{-1}/s^{-1})
dATP	13/20$_T$-mer[b]	100 ± 10[c,d]	10 ± 1[d]	1×10^7
dATP	13/20SP$_T$-mer	0.15 ± 0.01	35 ± 5	4300
dCTP	13/20SP$_T$-mer	0.008 ± 0.001	250 ± 50	32
dGTP	13/20SP$_T$-mer	0.023 ± 0.005	130 ± 20	180
dTTP	13/20SP$_T$-mer	0.055 ± 0.011	1200 ± 200	46

[a] Assays were performed using 1000 nM T4 exo$^-$ DNA polymerase, 250 nM DNA substrate, and variable concentrations of dNTP in the presence of 10 mM MgOAc. [b] Correct incorporation of dATP across from T was measured under pseudo-first-order reaction conditions. [c] This study. [d] Values reported by Frey et al. (*19*).

Inhibition by ddATP and ddGTP. In an attempt to alleviate complications in data analysis arising from extension beyond the abasic site, a series of single-turnover experiments were performed substituting ddGTP for dGTP. ddGTP is an isoteric analogue of dGTP and should be incorporated across from the abasic site in a manner identical to dGTP. However, since ddGTP is a chain-terminator, extension beyond the abasic site should not occur, and only 14-mer product should accumulate. Surprisingly, incorporation of ddGTP across from the abasic site did not occur at concentrations greater than 1 mM (data not shown).[3]

To evaluate if ddNTPs are competitive inhibitors, single-turnover experiments were performed in which the rate of dATP incorporation across from the abasic site was measured

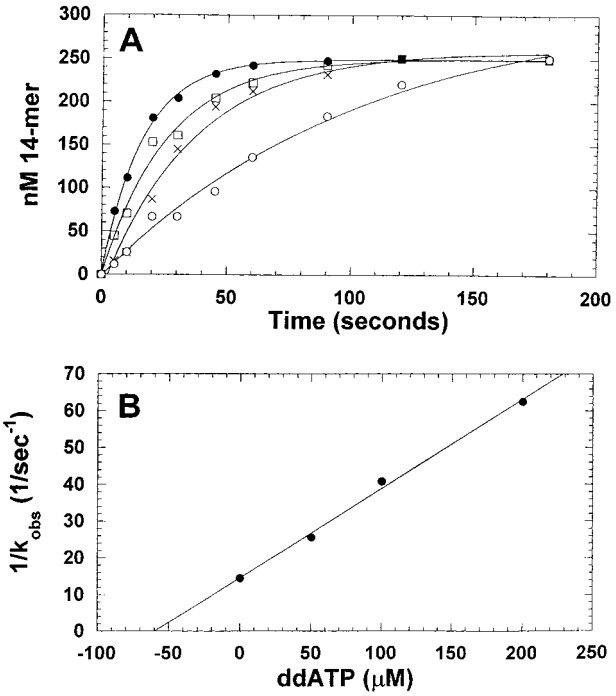

FIGURE 7: Inhibition of dATP incorporation by ddATP. (A) Time courses were generated by preincubating T4 exo$^-$ (1 μM) with 5′-labeled 13/20SP$_T$-mer (250 nM) followed by the addition of 0 (●), 50 (□), 100 (×), and 200 μM (○) ddATP. After a 5 s delay, 25 μM dATP was then added to initiate DNA synthesis. The reactions were quenched with 500 mM EDTA at variable times (5−300 s), and product formation was quantified by denaturing gel electrophoresis. The solid lines represent the fit of the data to a single exponential. (B) The reciprocal rate constants ($1/k_{obs}$) (●) were plotted versus the concentration of ddATP to yield an apparent K_i value for ddATP. The true K_i value for ddATP of 40 ± 5 μM was obtained as described in the text.

in the absence and presence of ddATP or ddGTP. The rate of dATP incorporation (14-mer production) was inhibited as the concentration of ddATP (Figure 7A,B) or ddGTP (data not shown) was increased. The true K_i value of 40 ± 10 μM for ddATP is nearly identical to the K_d value for dATP (35 μM). Likewise, the K_i value of 160 ± 30 μM for ddGTP is very similar to the measured K_d value of 130 μM for dGTP.

Elemental Effects during Polymerization Across from an Abasic Site. The elemental effect on DNA polymerization was determined using α-S-dNTP as the nucleotide triphosphate to determine if covalent bond formation contributes significantly to fidelity during translesion DNA synthesis (*14*, *25*). Table 3 summarizes the elemental effect (k^O/k^S) measured for the incorporation of dATP, dGTP, and dCTP obtained under pseudo-first-order or single-turnover conditions.

Extension beyond the Abasic Site. The ability of the DNA polymerase to extend beyond the abasic site was directly compared to that of extension beyond a mismatched 3′-termini. Under single-turnover conditions, dGTP incorporation across from T and beyond the formed G:T mismatch was rapid under the time frame tested (at least 5 s) such that the only product to significantly accumulate is 17-mer (Figure 8A). Because dGTP is the correct triphosphate for the next

[3] The lack of ddGTP incorporation may reflect perturbations in DNA polymerization activity induced by the abasic site. However, this is unlikely since the incorporation of ddATP was also not observed using unmodified 13/20$_T$-mer.

Table 3: Summary of Elemental Effects during Translesion DNA Synthesis

pseudo-first-order[a]		single-turnover[b]	
dNTP	k^O/k^S	dNTP	k^O/k^S
dATP	1.5 ± 0.2	dATP	1.1 ± 0.1
dCTP	1.7 ± 0.3	dCTP	1.9 ± 0.2
dGTP	3.5 ± 0.4	dGTP	3.1 ± 0.1
dTTP	ND[c]	dTTP	ND

[a] Assays performed under pseudo-first-order conditions used 10 nM T4 exo$^-$ DNA polymerase, 1000 nM DNA substrate, and K_m or 10 × K_m concentration of either α-O- or α-S-dNTP in the presence of 10 mM MgOAc. [b] Assays performed under single-turnover conditions used 1000 nM T4 exo$^-$ DNA polymerase, 250 nM DNA substrate, and K_m or 10 × K_m concentration of either α-O- or α-S-dNTP in the presence of 10 mM MgOAc. [c] Not determined.

three incorporations, the production of 17-mer is expected. By contrast, dGTP incorporation across from the abasic site and beyond the formed G:abasic site is significantly slower in which a mixture of polymerization products ranging from 15- to 17-mers accumulates (Figure 8B). The difference in banding patterns between dGTP incorporation across from T or an abasic site is illustrative of the differences in misincorporation and next correct incorporation. Using the simplified reaction mechanism depicted in Scheme 2, computer simulation was used to determine the rate and equilibrium constants that dictate product formation. Since single-turnover reaction conditions were employed, kinetic steps reflecting enzyme dissociation and rebinding to product DNA are assumed to be negligible. Thus, the rate and amount of product formation are dependent upon two parameters, the equilibrium dissociation constant (K_d) for dNTP and k_{pol}, the rate of DNA extension. k_{pol} was further simplified to combine the kinetic steps encompassing the conformational change prior to phosphoryl transfer, phosphoryl transfer, the conformational change after phosphoryl transfer, and pyrophosphate release. For initial computer simulations, the K_d value for dGTP was estimated at 150 μM using the K_m value for dGTP as well as the K_i value of ddGTP.

The data for product formation at 100 μM dGTP were initially used to obtain estimates for the parameters defining K_d and k_{pol} at each position in product formation. At this fixed concentration of dGTP, the time courses in product formation could be adequately fit either by maintaining values for K_d equal and varying k_{pol} (set A, Table 4) or by maintaining k_{pol} fixed and varying K_d (set B, Table 4). To evaluate which set of kinetic constants most accurately reflects the dynamics of replication beyond the abasic site, the rates and amount of product formation were measured as a function of varying concentrations of dGTP (10−1000 μM) (data not shown). Computer simulation was utilized to fit each data set using either set A or set B. The best global fit for the concentration dependency of dGTP was obtained using set A in which K_d was fixed at 200 μM and k_{pol} varied at each position in product formation (set A of Table 4).

The ability of the DNA polymerase to extend beyond an A:abasic site was evaluated under single-turnover conditions using the 14A/20SP-mer DNA substrate at varying concentrations of dGTP (50−1000 μM). Similar to data described above, extension beyond the A:abasic site displayed a mixture of products ranging from 15- to 17-mers (data not shown). The rate and amount of product formation were

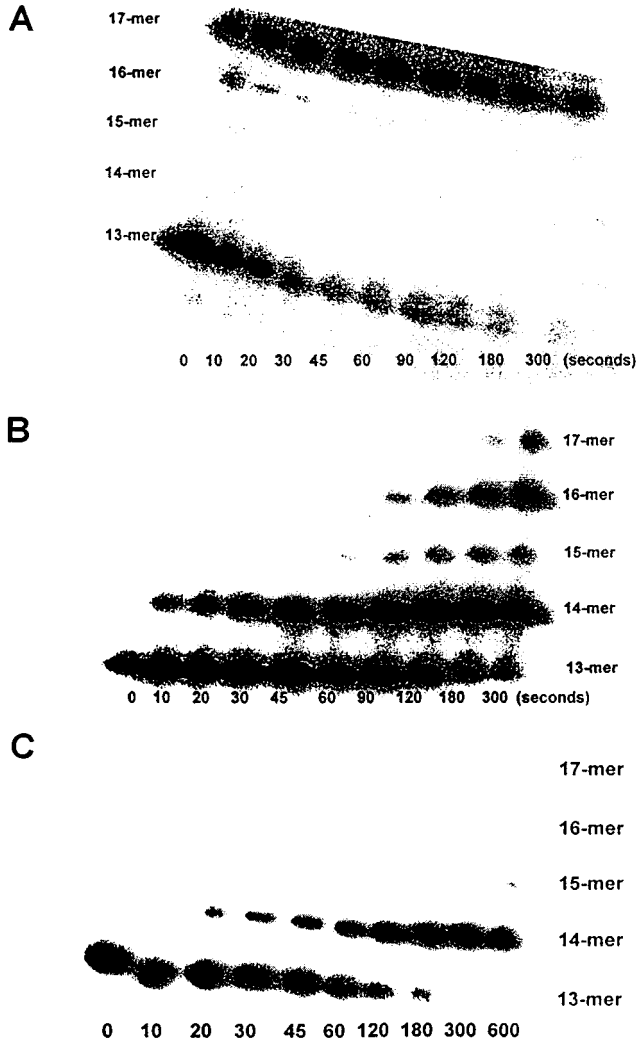

FIGURE 8: Comparison of misincorporation versus translesion DNA synthesis catalyzed by the exonuclease-deficient bacteriophage T4 DNA polymerase. (A) The time course for the misincorporation of dGTP across from T. (B) The time course for the incorporation of dGTP across from and beyond an abasic site. (C) The time course for the incorporation of α-S-dGTP across from and beyond an abasic site. Assays were performed in which T4 exo$^-$ polymerase (1 μM) and 5′-labeled DNA (250 nM) were preincubated, mixed with 100 μM dGTP or 100 μM α-S-dGTP to initiate the reaction, and quenched with 500 mM EDTA at variable times (5−180 s). The incorporation of dGTP was analyzed by denaturing gel electrophoresis. As noted in the text, because dGTP is the correct triphosphate for the next three incorporations, extension of a ladder of products ranging from 14 to 17 bases was observed.

Table 4: Kinetic Constants for dGTP Incorporation Across from and beyond an Abasic Site Catalyzed by T4 exo$^-$ DNA Polymerase[a]

	set A		set B	
position	K_d (μM)	k_{pol} (s^{-1})	K_d (μM)	k_{pol} (s^{-1})
13→14 (n+1)	200 ± 20	0.05 ± 0.01	200 ± 20	0.035 ± 0.005
14→15 (n+2)	200 ± 50	0.015 ± 0.005	1400 ± 50	0.065 ± 0.005
15→16 (n+3)	200 ± 30	0.12 ± 0.01	20 ± 5	0.05 ± 0.01
16→17 (n+4)	200 ± 25	0.015 ± 0.005	2000 ± 150	0.045 ± 0.010

[a] Rate and equilibrium constants were obtained using computer simulation to fit the time courses of product formation as a function of dGTP concentration. See text for further discussion.

dependent upon dGTP concentration. As before, computer simulation of each data set was used to obtain the values of K_d and k_{pol} summarized in Table 5. For comparison, the average values for k_{pol} and K_d obtained for extension beyond a G:abasic site are also provided.

Single-turnover assays were also performed to evaluate the ability of the DNA polymerase to extend beyond a C:abasic site. At the highest concentration of dGTP tested (1 mM), extension from 14C/20SP-mer displayed only accumulation of 14-mer (n+1) (data not shown). The time course extension was linear as opposed to the single exponentials obtained for extension beyond a G:abasic site or A:abasic site. A steady-state rate of 1.3 ± 0.1 nM/s was obtained.

Elemental Effects on Incorporation beyond an Abasic Site. The elemental effect on the rate of extension beyond the abasic site was directly measured using 13/20SP-mer substituting α-S-dGTP for α-O-dGTP. In these experiments, the rates and amount of product formation were measured by varying the concentration of α-S-dGTP from 25 to 1000 μM. In general, utilization of α-S-dGTP slows the rate of each incorporation event as compared to that using α-O-dGTP. The best global fit for the concentration dependency of α-S-dGTP was obtained using the parameters in which K_d was maintained at approximately 200 μM while k_{pol} varied at each position in product formation. Average values for k_{pol} and K_d are summarized in Table 5. Comparison of the elemental effects at each position reveals a small elemental effect of 3.7 for incorporation across from the abasic site (n+1). However, larger elemental effects of 5.6 and 10.6 are obtained for the conversion of 14-mer to 15-mer (n+2) and 15-mer to 16-mer (n+3), respectively, suggesting that phosphoryl transfer is at least partially rate-limiting for incorporation beyond the abasic site. The lack of appreciable extension of the 16-mer into 17-mer (n+4) with α-S-dGTP precludes accurate determination of values for k_{pol}, and thus an elemental effect at this position cannot be measured.

The elemental effect on the rate of extension beyond an A:abasic site was also evaluated by varying the concentration of α-S-dGTP (data not shown). As before, global fit analysis was utilized to obtain average values for k_{pol} and K_d (summarized in Table 5). Large elemental effects of 4.7 and 20.3 are obtained for the conversion of 14-mer to 15-mer (n+2) and 15-mer to 16-mer (n+3), respectively. Surprisingly, appreciable extension of the 16-mer into 17-mer (n+4) was observed by substituting α-S-dGTP for α-O-dGTP. The minimal elemental effect of 1.6 suggests that phosphoryl transfer is not rate-limiting for incorporation at this position.

Determination of the Equilibrium Dissociation Constant, K_d, of 13/20SP-mer for the Exonuclease-Deficient DNA Polymerase. The binding affinity of the DNA polymerase for the modified DNA primer/template was directly assessed by determining the equilibrium dissociation constant (K_d) of enzyme for 13/20SP-mer. In these experiments, the polymerization reaction was monitored using a constant amount of T4 exo$^-$ polymerase (100 nM) and variable amounts of 13/20SP$_T$-mer (12.5−200 nM). At DNA concentrations less than 100 nM, the observed burst of single-nucleotide incorporation at low DNA concentrations is consistent with rapid elongation of the T4 exo$^-$:13/20SP$_T$-mer complex, and the amplitude of the burst is a measure of the level of this complex. At DNA concentrations greater than 100 nM, bursts in product formation are also observed. Under these second-order reaction conditions, the observed burst amplitudes likely reflect substrate depletion. The burst amplitudes were

Table 5: Kinetic Constants for α-O-dGTP and α-S-dGTP Incorporation Across from and beyond an Abasic Site Catalyzed by T4 exo⁻ DNA Polymerase[a,b]

position	α-O-dGTP		α-S-dGTP		elemental effect,[c]
	K_d (μM)	k_{pol} (s^{-1})	K_d (μM)	k_{pol} (s^{-1})	k^O/k^S
			13/20SP-mer		
13→14 (n+1)	200 ± 20	0.051 ± 0.012	200 ± 25	0.014 ± 0.007	3.7
14→15 (n+2)	200 ± 50	0.014 ± 0.004	200 ± 30	0.0025 ± 0.0003	5.6
15→16 (n+3)	200 ± 30	0.117 ± 0.005	200 ± 25	0.011 ± 0.003	10.6
16→17 (n+4)	200 ± 25	0.016 ± 0.005	ND	ND	
			14A/20SP-mer		
14→15 (n+2)	240 ± 15	0.28 ± 0.05	240 ± 25	0.059 ± 0.008	4.7
15→16 (n+3)	160 ± 20	0.65 ± 0.13	170 ± 30	0.032 ± 0.011	20.3
16→17 (n+4)	200 ± 2	0.06 ± 0.01	210 ± 20	0.038 ± 0.015	1.6

[a] Assays performed under single-turnover conditions used 1000 nM T4 exo⁻ DNA polymerase, 250 nM DNA substrate, and varying concentrations of either α-O- or α-S-dGTP in the presence of 10 mM MgOAc. [b] Rate and equilibrium constants were obtained using computer simulation to fit the time courses of product formation as a function of dGTP concentration. See text for further discussion. [c] The elemental effect, k^O/k^S, on nucleotide incorporation was obtained by taking the ratio of the rate constant for incorporation using α-O-dGTP versus the rate constant for incorporation using α-S-dGTP.

Scheme 3: Kinetic Mechanism for the Bacteriophage T4 DNA Polymerase[a]

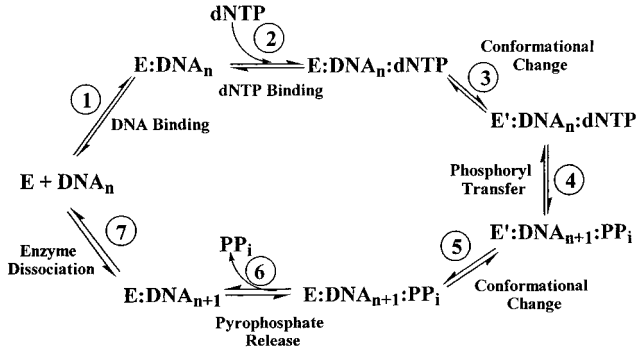

[a]Individual steps along the pathway for DNA polymerization are numbered and identified. Abbreviations: E = T4 DNA polymerase, DNA_n = DNA substrate, E′ = conformational change in DNA polymerase, PP_i = inorganic pyrophosphate, and DNA_{n+1} = DNA product (DNA extended by one nucleobase).

fit to the quadratic equation to yield a K_d of 50 ± 10 nM, which is comparable to the value of 40 nM reported for the T4 exo⁻ polymerase using unmodified $13/20_T$-mer (*19*, *26*).

DISCUSSION

DNA polymerization proceeds via a multistep kinetic process (Scheme 3), the overall complexity of which is invoked to preserve fidelity during nucleotide incorporation. In this report, the mechanism and dynamics of translesion DNA synthesis were evaluated using the bacteriophage T4 exonuclease-deficient DNA polymerase as a model system to examine which kinetic step is primarily responsible for hindering replication across from and beyond an abasic site. T4 exo⁻ DNA polymerase is capable of incorporating each triphosphate across from the abasic site although a definitive preference for dATP incorporation is observed. Although not exhaustively tested, the preferential incorporation of dATP appears to be relatively insensitive to DNA sequence. Steady-state parameters (Table 1) indicate that the k_{cat}/K_m for dATP is 18-fold higher than that of dGTP and approximately 50-fold higher than dTTP and dCTP. Surprisingly, dATP incorporation across from the abasic site is only 220-fold less efficient than precise DNA replication of incorporation of dATP across from dT (vida supra, *11, 19*) under steady-state conditions. The decrease in catalytic efficiency appears to arise primarily from the 25-fold decrease in k_{cat}. However, direct comparison of the k_{cat} values is misleading since in the case of correct incorporation, k_{cat} reflects release of enzyme from extended DNA substrate during precise DNA replication (*11*). The inequality in k_{cat} values for translesion DNA synthesis (Table 1) suggests that release of enzyme from product DNA may no longer be rate-limiting for enzyme turnover. The change in rate-limiting step was confirmed through pre-steady-state kinetic analysis of the time course in nucleotide incorporation as a function of dNTP. Incorporation of dATP or dGTP across from the abasic site was linear whereas the kinetics of single-nucleotide incorporation with dTTP and dCTP showed small but definitive lags followed by a linear steady-state rate. These data alone indicate that chemistry or a step prior to chemistry is rate-limiting for translesion DNA synthesis. However, the small elemental effects (<2) observed under pseudo-first-order reaction conditions place the rate-limiting step prior to chemistry. A formal possibility to explain the altered kinetics of incorporation is that the binding of polymerase to abasic-containing DNA substrates is significantly perturbed. This possibility appears unlikely as the K_d for 13/20SP-mer is essentially equal to that of unmodified 13/20-mer. Furthermore, pre-steady-state analysis reveals that the kinetics of dATP incorporation prior to encountering the abasic site are unperturbed, i.e., a full burst amplitude in product formation coupled with a polymerization rate constant of ~100 s^{-1}. Collectively, these data suggest that the polymerase cannot "sense" the DNA lesion to cause the observed perturbations in the dynamics of nucleotide incorporation. Thus, either ground-state binding of the incoming dNTP and/or the conformational change preceding chemistry limits the overall rate of incorporation.

Values for k_{pol} and K_d for each dNTP (Table 2) were measured through a series of single-turnover experiments. While k_{pol} values are dependent upon the dNTP utilized, they are essentially equal to the corresponding k_{cat} values and provide evidence that the conformational change preceding phosphoryl transfer is the rate-limiting step for nucleotide incorporation. The minimal elemental effect (<2-fold) observed using α-S-dATP or α-S-dCTP under single-turnover conditions again argues that the conformational change preceding chemistry is the rate-limiting step for incorporation. If correct, then rapid equilibrium binding of

dNTP to the Pol:DNA complex must exist such that the K_m values measured under pseudo-first-order conditions should equal K_d. This is true in the case of dATP, dCTP, and dTTP as the measured K_m and K_d values are identical within experimental error. Furthermore, the K_i value of 40 μM for ddATP, a competitive inhibitor, is nearly identical to the K_d value of dATP (35 μM) and is consistent with rapid equilibrium ground-state binding followed by a rate-limiting step preceding chemistry. It is noted that the measured K_d for dGTP is approximately 2-fold lower than its K_m value. However, the K_i value of 160 μM for ddGTP is nearly identical to the K_d value of 130 μM for dGTP and likely represents the intrinsic binding affinity of dGTP across from the abasic site. The higher K_m value may reflect the contribution of chemistry toward the rate-limiting step during catalysis using dGTP as the substrate, and this is consistent with the slightly larger elemental effect (~3-fold) measured under pseudo-first-order conditions.

The data thus far indicate that the kinetic mechanisms of correct and translesion DNA replication are essentially identical although the dynamics of the kinetic pathway are significantly different. Specifically, ground-state binding (step 2 in Scheme 3) and the conformational change (step 3 in Scheme 3) are highly disfavored during translesion DNA synthesis. However, it is the conformational change preceding chemistry that not only limits nucleotide incorporation but also limits enzyme turnover. This contrasts significantly with the dynamics of correct incorporation in which release of enzyme from product DNA is the rate-limiting step for enzyme turnover (*11*, *19*). The change in rate-limiting step for enzyme turnover makes an accurate comparison of k_{cat}/K_m values impossible. However, since the conformational change is rate-limiting for nucleotide incorporation in either case and reflects k_{pol}, a direct comparison of catalytic efficiency can be made from evaluating k_{pol}/K_d values. The catalytic efficiency of correct incorporation of dATP is approximately 10^7 M^{-1} s^{-1} while that for the incorporation of dATP across from an abasic site is 4.3×10^3 M^{-1} s^{-1}. This corresponds to a mere 2300-fold reduction in catalytic efficiency. Surprisingly, the decrease in catalytic efficiency arises primarily from a modest reduction in the rate of the conformational change (~700-fold) and only a minimal change in ground-state binding for dATP (~3-fold). These results contrast significantly with those obtained for DNA polymerase α in which the K_m for dATP increased 1000-fold during incorporation across from an abasic site as compared to incorporation from T while V_{max} was essentially unaffected (*27*). A more dramatic effect on replication efficiency is observed for the incorporation of the other nucleoside triphosphates. Specifically, incorporation of dGTP is reduced by a factor of 56 000 while incorporation of dCTP or dTTP is reduced by a factor of 310 000 or 220 000, respectively. While a reduction in binding affinity plays a role in discriminating against the incorporation of these dNTPs, it is the conformational change that plays the predominant role as this step is reduced by 3−4 orders of magnitude compared to precise DNA replication.

The perturbations in ground-state dNTP binding coupled with substantial reductions in the rate of the conformational change preceding chemistry are consistent with the induced-fit model (*14*) for controlling the maintenance of DNA fidelity during replication. In the context of an induced-fit model, the conformational change is viewed as a substrate selection gate in which initial loose binding of the correct substrate triggers a conformational change leading to an active configuration of the enzyme. Transition-state stabilization for catalysis is provided when key residues within the active site are brought into proper alignment after the conformational change. In contrast, binding of the incorrect substrates during mispair formation results in an inappropriate fit such that the conformational change occurs at a slower rate. Since an abasic site is devoid of any potential hydrogen-bonding interactions with an incoming dNTP, it is reasonable that all dNTPs appear to be recognized as relatively poor substrates, and this is reflected in their slow rates of incorporation.

However, if proper base pairing alone "triggers" the conformational change, then why is the rate of the conformational change dNTP-dependent during incorporation across from the abasic site? The lack of hydrogen-bonding capabilities of the abasic site predicts that all four dNTPs should be incorporated with equal efficiency. However, this is not the case as k_{pol} values vary by at least 20-fold. One reasonable explanation for the inequality in nucleotide incorporation is provided from recent NMR studies evaluating the relative stability of the four nucleosides across from an abasic site (*17*, *18*). These studies reveal that when dAMP is opposite an abasic site, the nucleobase is stacked in an intrahelical configuration which causes minor distortion of the DNA helix. dGMP appears to be either inter- or extrahelical while dCMP and dTMP are poorly stacked and are found to be extrahelical. Thus, a dAMP:abasic site pair can be considered to be more thermodynamically favored than the other potential pairs. The kinetic data presented here may be interpreted with regard to this structural information. The 100-fold higher efficiency of dATP incorporation may result from this nucleoside triphosphate being stacked in an intrahelical configuration causing minor distortion of the DNA helix. In this configuration, the polymerase binds dATP with higher affinity and overcomes the energy barrier associated with the conformational change much easier than with the other dNTPs that are likely to be bound in an extrahelical configuration.

Consistent with this argument is the fact that mismatch DNA synthesis is distinctly favored over replication across from an abasic site. Direct comparison of k_{cat}/K_m values (Table 1) reveals a ~5-fold higher efficiency in mismatch DNA synthesis compared to incorporation across an abasic site.[4] At face value, this suggests that the lack of hydrogen-bond capabilities has a more negative effect on replication efficiency than the creation of aberrant hydrogen bonds. However, although the Watson−Crick base pair geometry is violated in forming a mismatched base pair, there is no significant local perturbation of the helix, and the global conformation of the duplex is unaffected (*28*). This contrasts significantly with the observed local perturbations in the DNA helix structure of DNA duplexes containing dGMP, dCMP, and dTMP across from an abasic site (*17*, *18*).

These perturbations in the DNA helix may also explain the difficulty in extension beyond a dNMP:abasic site

[4] A direct comparison of k_{cat}/K_m values can be made in this instance since k_{cat} is limited by the conformational change preceding chemistry in both cases.

mispair. Specifically, extension beyond a G:T mismatch is extremely efficient under single-turnover conditions as exemplified by the rapid and successive incorporation beyond the G:T mispair to yield only fully elongated 17-mer. By contrast, extension beyond a G:abasic site is substantially slower in which a distribution of products ranging from 14- to 17-mers is obtained under identical reaction conditions. The faster rates of correct incorporation likely reflect the more favorable configuration of a G:T mismatch compared to a G:abasic site mispair. By contrast, dAMP is stacked in an intrahelical configuration which is expected to be in a more favorable configuration for extension. Consistent with this hypothesis, the rates of extension from an A:abasic site are at least 20-fold faster at position $n+1$ and approximately 3.5-fold faster at positions $n+2$ and $n+3$, respectively, as compared to a G:abasic site mispair. Furthermore, extension beyond a C:abasic mispair, which exists in an extrahelical configuration, is severely retarded as reflected by the approximately 100-fold slower rate in $n+1$ production compared to extension beyond an A:abasic site mispair. Collectively, these data argue that the efficiency of extension beyond a dNMP:abasic site is modulated by whether the terminal base pair is inter- or extrahelical.

Another surprising feature of translesion replication is the apparent long-range effects on replication efficiency by perturbations in the DNA helix induced by the presence of an abasic site. The difference in rates of extension beyond a G:abasic site or A:abasic site mispair is illustrative of the differences in the kinetics of next correct incorporation. The decrease in catalytic efficiency could result from several factors. As a G:abasic site mispair adversely affects the local structure of the DNA, it is possible that the affinity of enzyme for this DNA substrate is greatly reduced, causing the enzyme to preferentially dissociate rather than incorporate. This is unlikely since experiments performed using a molar excess of enzyme versus DNA should overcome reduced binding affinity of polymerase for DNA. More convincing is the concentration dependency of dGTP on the rates and extent of product formation which argue against enhanced dissociation but instead reflect perturbations in a step associated with ground-state dNTP binding, the conformational change preceding chemistry and/or chemistry itself. Data summarized in Table 5 indicate that the K_d of dGTP is 200 μM regardless of potential incorporation position. Furthermore, the K_d for dGTP is identical regardless of whether extension occurs from an A:abasic or G:abasic site mispair; the differences in the kinetics of next correct incorporation do not reflect alterations in ground-state binding but may reflect perturbations in the conformational change preceding chemistry and/or chemistry.

To evaluate which kinetic step was rate-limiting for extension beyond a dNMP:abasic mispair, the elemental effect on DNA polymerization was determined using α-S-dGTP as the nucleotide triphosphate. Extension from the G:abasic site mispair generates significant elemental effects of 5.6 and 10.6 for the conversion of 14-mer to 15-mer ($n+2$) and 15-mer to 16-mer ($n+3$), respectively, suggesting that phosphoryl transfer is at least partially rate-limiting for incorporation at these positions. Similar elemental effects of 4.7 and 20.3 are obtained at positions $n+2$ and $n+3$, respectively, for extension from an A:abasic site mispair. The similarity in the elemental effects argues than the rate-limiting step for extension beyond a dNMP:abasic site mispair is chemistry rather than the conformational change preceding chemistry. Furthermore, the similarity in the elemental effects indicates that the change in rate-limiting step is independent of whether extension is from a G:abasic or A:abasic site.

CONCLUSION

Nucleotide incorporation across from an abasic site is limited by the conformational change preceding chemistry while extension beyond a dNMP:abasic site is limited by chemistry. In both instances, the dynamics of each process appear to be predominantly controlled by the relative configuration of the dNMP:abasic site mispair. Consistent with this mechanism is the fact that the rates of incorporation across from and beyond the abasic site are faster using dATP. Although dATP is the preferred nucleobase for insertion across from the abasic site, the magnitude of 2300-fold reduction in catalytic efficiency is very low and suggests that other kinetically discrete steps outlined in Scheme 1 may participate in the prevention of translesion DNA synthesis. Enzyme dissociation from the altered DNA substrate could arguably play a role in preventing translesion DNA synthesis since the rate of incorporation across from an abasic site is between 10- and 250-fold slower than the rate of enzyme dissociation from unmodified DNA (*19*, *26*). However, it is important to recognize that during in vivo DNA replication, the T4 DNA polymerase is complexed with its respective accessory proteins (*29*). These accessory proteins reduce the rate of enzyme dissociation from 2 s^{-1} to approximately 0.1 s^{-1} (*30*), a time frame in which extension across from and beyond an abasic site could take place. The effect of increased processivity toward enhancement of translesion DNA synthesis will prove to be an interesting area of inquiry and is currently being evaluated. A more likely mechanism is that the slow rate of extension beyond the site of DNA damage allows access of the mispair to the enzyme's exonuclease site to remove the aberrant base pair. Indeed, steady-state analysis using the wild-type T4 DNA polymerase (exonuclease-proficient) reveals that dATP is not stably incorporated across from the abasic site even at concentrations greater than 1 mM (unpublished data, A.J.B.). Presumably, the enzyme partitions between polymerase and exonuclease active sites to prevent the stable insertion of a nucleobase across from the abasic site. It will prove interesting to evaluate the dynamics of exonuclease activity and idle turnover in the context of translesion DNA synthesis.

REFERENCES

1. Loeb, L. A., and Preston, B. D. (1986) *Annu. Rev. Genet. 20*, 201−230.
2. Mol, C. D., Parikh, S. S., Putnam, C. D., Lo, T. P., and Tainer, J. A. (1999) *Annu. Rev. Biophys. Biomol. Struct. 28*, 101−128.
3. Lindahl, T. (1993) *Nature 362*, 709−715.
4. Breen, A. P., and Murphy, J. A. (1995) *Free Radical Biol. Med. 18*, 1033−1077.
5. Krokan, H. E., Nilsen, H., Skorpen, F., Otterlei, M., and Slupphaug, G. (2000) *FEBS Lett. 476*, 73−77.
6. Gentil, A., Renault, G., Madzak, C., Margot, A., Cabral-Neto, J. B., Vasseur, J. J., Rayner, B., Imbach, J. L., and Sarasin, A. (1990) *Biochem. Biophys. Res. Commun. 173*, 704−710.

7. Schaaper, R. M., Kunkel, T. A., and Loeb, L. A. (1983) *Proc. Natl. Acad. Sci. U.S.A. 80*, 487−491.
8. Boiteux, S., and Laval, J. (1982) *Biochemistry 21*, 6746−6751.
9. Efrati, E., Tocco, G., Eritja, R., Wilson, S. H., and Goodman, M. F. (1997) *J. Biol. Chem. 272*, 2559−2569.
10. Schaaper, R. M. (1993) *J. Biol. Chem. 268*, 23762−23765.
11. Capson, T. L., Peliska, J. A., Kaboord, B. F., Frey, M. W., Lively, C., Dahlberg, M., and Benkovic, S. J. (1992) *Biochemistry 31*, 10984−10994.
12. Kuchta, R. D., Benkovic, P. A., and Benkovic, S. J. (1988) *Biochemistry 27*, 6716−6725.
13. Eger, B. T., Kuchta, R. D., Carroll, S. S., Johnson, K. A., Benkovic, P. A., and Benkovic, S. J. (1991) *Biochemistry 30*, 1441−1448.
14. Wong, I., Patel, S. S., and Johnson, K. A. (1991) *Biochemistry 30*, 526−537.
15. Donlin, M. J., Patel, S. S., and Johnson, K. A. (1991) *Biochemistry 30*, 538−546.
16. Mendelman, L. V., Petruska, J., and Goodman, M. F. (1990) *J. Biol. Chem. 265*, 2338−2346.
17. Cuniasse, Ph., Sowers, L. C., Eritja, R., Kaplan, B., Goodman, M. F., Cognet, J. A. H., LeBret, M., Guschlbauer, W., and Fazakerley, G. V. (1987) *Nucleic Acids Res. 15*, 8003−8022.
18. Cuniasse, Ph., Fazakerley, G. V., Guschlbauer, W., Kaplan, B. E., and Sowers, L. C. (1987) *J. Mol. Biol. 213*, 303−314.
19. Frey, M. W., Nossal, N. G., Capson, T. L., and Benkovic, S. J. (1993) *Proc. Natl. Acad. Sci. U.S.A. 90*, 2579−2583.
20. Johnson, K. A. (1995) *Methods Enzymol. 249*, 38−61.
21. Mizrahi, V., Benkovic, P. A., and Benkovic, S. J. (1986) *Proc. Natl. Acad. Sci. U.S.A. 83*, 5769−5773.
22. Barshop, B. A., Wren, R. F., and Frieden, C. (1983) *Anal. Biochem. 130*, 134−145.
23. Kroutil, L. C., Frey, M. W., Kaboord, B. F., Kunkel, T. A., and Benkovic, S. J. (1998) *J. Mol. Biol. 278*, 135−146.
24. Sagher, D., and Strauss, B. (1983) *Biochemistry 22*, 4518−4526.
25. Herschlag, D., Piccirilli, J. A., and Cech, T. R. (1991) *Biochemistry 30*, 4844−4854.
26. Berdis, A. J., Soumillion, P., and Benkovic, S. J. (1996) *Proc. Natl. Acad. Sci. U.S.A. 93*, 12822−12827.
27. Randall, S. K., Eritja, R., Kaplan, B. E., Petruska, J., and Goodman, M. F. (1987) *J. Biol. Chem. 262*, 6864−6870.
28. Hunter, W. N., Brown, T., Kneale, G., Anand, N. N., Rabinovich, D., and Kennard, O. (1987) *J. Biol. Chem. 262*, 9962−9970.
29. Sexton, D. J., Berdis, A. J., and Benkovic, S. J. (1997) *Curr. Opin. Chem. Biol. 1*, 316−322.
30. Kaboord, B. F., and Benkovic, S. J. (1996) *Biochemistry 35*, 1084−1092.

BI0101594